

Size-strain analysis using the fundamental parameter (FP) method

Akihiro Himeda*

1. Background

Crystallite size and strain affect the physical (mechanical, electric, magnetic and optical) properties of materials. It is quite important to quantify size and strain, and to clarify the relationship between them in the field of material science.

The effects of finite crystallite size and lattice strain can be observed as deformations in the shape of diffraction curves. Thus, information can be obtained by investigating their shapes. However, the deformation occurs due to not only size-strain effects but also instrumental effects.

In conventional estimation, only the width of the peaks is used, not the whole peak shape. To eliminate the instrumental effect, width correction is carried out by measuring standard samples and subtracting the breadths of peaks of the width standard sample from those of a sample being investigated. With the 2-theta dependence of the corrected peak width, we can extract the crystallite size and lattice strain quantities.

However, the method of subtraction depends on whether the peak shape is assumed to be Gaussian or Lorentzian. In addition to this, the peak shape will not necessarily express a Gaussian or Lorentzian function. Moreover, so-called “super Lorentzian” peak shapes are reported for samples with broader distribution of crystallite size. Based on this, applied width corrections may have limited validity.

In contrast to the above, the fundamental parameter method (FP method)⁽¹⁾ has recently been used to analyze the effect of profile shape originated from instrumental conditions. In the FP method, the peak shape is calculated by convoluting the instrumental profile shapes assuming a theoretical model of instrument and profiles originated from crystallite size and lattice strain. In this way, we can obtain size-strain information and eliminate the instrumental effects without measuring standard samples.

Size distribution can also be quantified by analyzing the precise peak shape. Size distribution affects the sharpness close to the peak top and slow fading off of its tails.

In PDXL 2⁽²⁾, crystallite size, size distribution and strain can be analyzed with the FP method more easily than the ordinary Rietveld method. In this report, theoretical background to analyze them and some

applications of actual samples using PDXL are described.

2. Crystallite size, size distribution and strain

X-ray profile diffracted from a spherical crystallite with its diameter D is expressed as⁽³⁾,

$$f_s(k; D) = \frac{3D}{s^2} \left[1 - \frac{2}{s} \sin s + \frac{4}{s^2} \sin^2 \left(\frac{s}{2} \right) \right]$$

Here,

$$s = 2\pi kD$$

and

$$k = 2(\sin(\theta + \Delta\theta) - \sin\theta) / \lambda \cong 2\Delta\theta \cos\theta / \lambda$$

Since actual powder samples consist of a lot of crystallites with varied diameters, the observable profile shape is formulated with an averaged function by the distribution function P of their diameters as:

$$f_s(k; D_0, C) = \int_0^\infty dD f_s(k; D) P(D; D_0, C)$$

Lognormal distribution is widely used for the distribution function. It is known that the size distribution obtained by means of electron microscopy is often closely lognormal. The function form is expressed as:

$$P(D; D_0, C) = \frac{1}{D\sqrt{2\pi \ln(1+C^2)}} \exp \left[-\frac{\left\{ \ln \left((D/D_0) \sqrt{1+C^2} \right) \right\}^2}{2\ln(1+C^2)} \right]$$

Here, D_0 is a volume weighted mean diameter and C is a normalized standard deviation which expresses the broadness of the distribution. In Fig. 1, profile shape dependences in terms of C are shown. The red line shows the profile when $C=0.1$, assuming very narrow distribution of diameters, which is almost identical to that of a single spherical crystallite. As the distribution becomes broader ($C=1$ in green line and $C=1.5$ in blue line), the shape near the peak top becomes sharper and its tail trails more slowly. Since these three profiles have the same volume weighted mean diameter value, their peak widths do not correspond to the average diameter. This means the conventional size analysis used the peak breadth is quantitatively insufficient.

* Application & Software Development Department, X-ray Analysis Division, Rigaku Corporation.

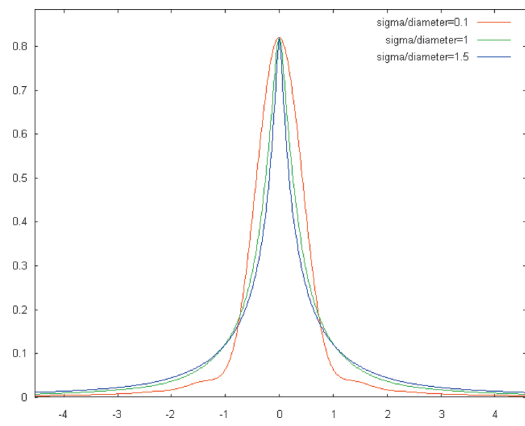


Fig. 1. Distribution width C dependences of the profile shape.

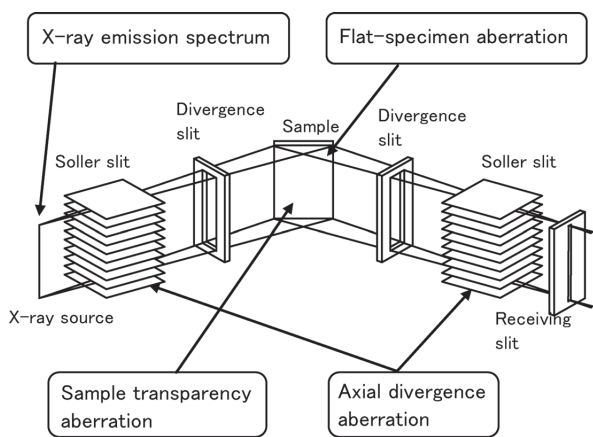


Fig. 2. Schematic diagram of a Bragg-Brentano diffractometer.

3. FP method

In the FP method, an observed profile is obtained by convoluting the profile from crystallites described in the previous section and those from instrumental aberration functions. In the case of Bragg-Brentano diffractometers, which are widely used for powder diffractometry, the instrumental functions are listed as follows:

- a. X-ray emission spectrum
- b. axial divergence aberration
- c. receiving-slit width function
- d. flat-specimen aberration
- e. sample-transparency aberration
- f. effective focus size

Typical profile shapes from the above aberration functions are shown in Fig. 3. Profile changes with convoluting aberration functions are shown in Fig. 4. Crystallite profile is given in red. Profiles from successively applied convolutions of emission spectrum, axial divergence, receiving-slit width, flat-specimen, sample-transparency, and effective focus size are shown in green, blue, pink, dark blue and brown, respectively. It is shown that the dominant effects in this case are from emission spectrum and axial divergence aberration.

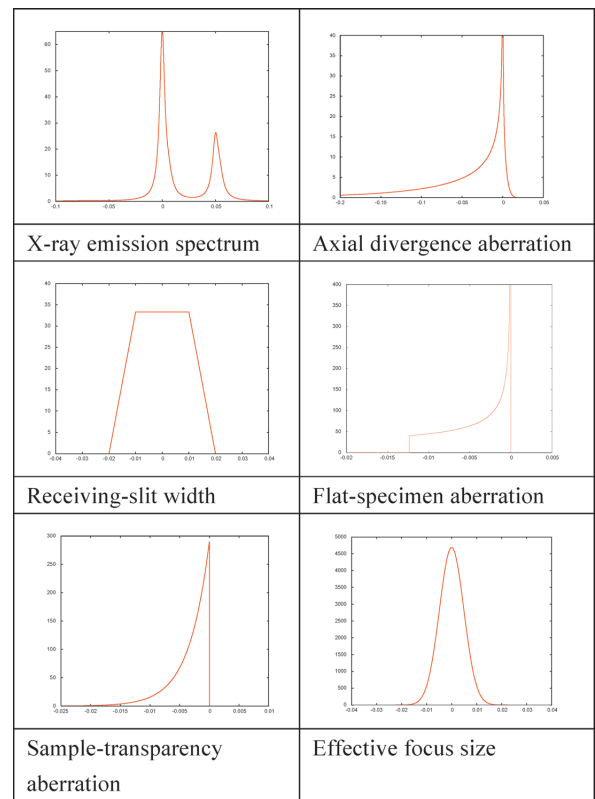


Fig. 3. Typical profile shapes for each instrumental aberration function.

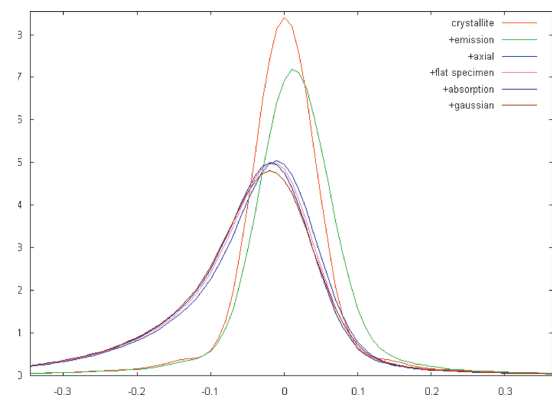


Fig. 4. Convolution of instrumental aberration functions.

Precise values of crystallite size, size distribution and strain are obtained by the least-square fitting to the measurement using the final profile convoluted all instrumental functions.

Although this convolution method itself is equivalent to that in the Rigaku software package, CSDA⁽⁴⁾, which can analyze crystallite size distribution, we apply a much faster convolution algorithm developed by R. W. Cheary *et al.* in PDXL that has achieved analysis times about fifty times faster than CSDA. Thus, we can apply this method to whole pattern fitting analysis and can obtain much reliable results compared with those by CSDA which analyzes only a single peak. In addition, lattice strain e , which cannot be refined using CSDA, can also be obtained simultaneously. In the next

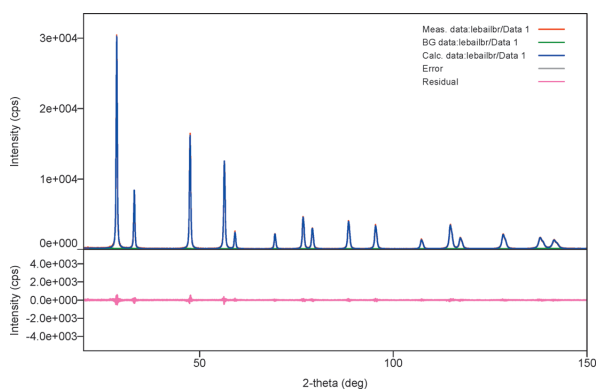


Fig. 5. Profile refined with the Pawley decomposition.

section, application examples using actual observations are shown.

4. Application

4.1. Size-strain round robin

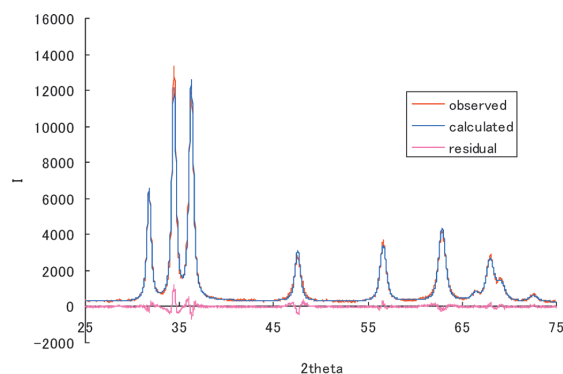
The commission on Powder Diffraction of the International Union of Crystallography held a size-strain round robin and published the results⁽⁵⁾. We analyzed one of the supplied data sets taken using Bragg-Brentano geometry in the University of Maine, among the observed data using PDXL. The Pawley decomposition, which treats the integrated intensities of diffraction lines as refinable parameters, is applied to the data. The refined profile is shown in Fig. 5. Red, blue and pink lines show measured profile, theoretical profile and their residuals, respectively. Figures of the refinement are $R_{wp}=5.96\%$ and $S=1.412$. The results give a volume averaged mean diameter of 30.16(4) nm, normalized size distribution deviation of 0.411(2) and lattice strain of 0.027(2)%. In the report of the round robin, diameter and its distribution deviation are summarized in Tables 2 and 3. Results in Table 2 are obtained with profile fitting to the deconvoluted profile by Richardson algorithm. D_V in the paper is called “apparent domain size” and defined the next formula⁽⁶⁾.

$$D_V = \frac{1}{V} \iiint t \, dx \, dy \, dz$$

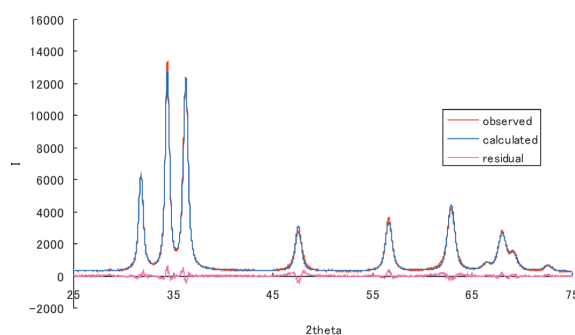
Here, V is the volume of a crystallite and t is the thickness of a crystallite parallel to the diffraction vector through (x, y, z) . Applying this to a spherical crystallite with diameter D , we obtain,

$$D_V = 3D/4.$$

With this formula, volume weighted mean diameter $D=30.16(4)$ nm is converted to $D_V=22.62(3)$ nm, which is almost the same as the reported value. Square of the size distribution deviation C corresponds to the dispersion c and the value 0.169(2) is only slightly smaller than the reported value. In addition, the results of the Warren-Averbach analysis are summarized in Table 3 of the report. The results show that the correlation between strain and size distribution is



(a)



(b)

Fig. 6. Pawley fitting assuming (a) spherical crystallite and (b) ellipsoidal crystallite for ZnO nanocrystalline.

relatively strong and that it is difficult to separate them. In PDXL, it is realized by refining both parameters simultaneously using the whole profile pattern.

4.2. Application to sample with anisotropic crystallite

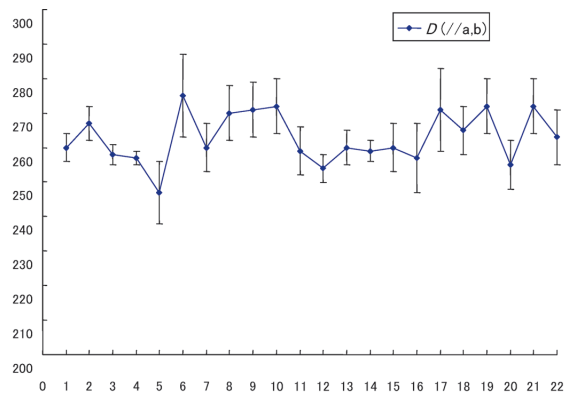
Next, we show an analysis of an anisotropic crystallite. When a crystallite has anisotropy, its diameter depends on the Miller indices. Assuming ellipsoidal shape for a crystallite, the (h, k, l) dependence of the diameter is given as⁽⁸⁾,

$$\frac{1}{D_h^2} = \frac{hD_{sq}^{-1}h}{hh} = \frac{b_1h^2 + b_2k^2 + b_3l^2 + 2b_2hk + 2b_3hl + 2b_23kl}{h^2a^{*2} + k^2b^{*2} + l^2c^{*2} + 2hka^*b^*\cos\gamma^* + 2hla^*c^*\cos\beta^* + 2klb^*c^*\cos\alpha^*}$$

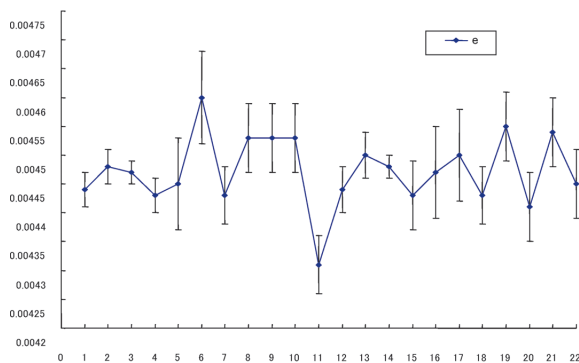
Here we analyze a measurement of the ZnO nanocrystalline material using Bragg-Brentano geometry. In Fig. 6(a), the refined profile assuming spherical crystallites is plotted ($R_{wp}=6.53\%$, $S=1.65$ and $D=30.9$ nm). The residual plot around the second and third peaks indicates the existence of anisotropy in the crystallite, because the second theoretical peak is sharper and the third theoretical peak is broader than those of the observed peaks. In Fig. 6(b), the refined profile assuming ellipsoidal crystallites is shown ($R_{wp}=6.31\%$, $S=1.595$, $D=25.9$ nm in a, b -axis direction and $D=33.8$ nm in c -axis direction). Since the residual is decreased when an anisotropic crystallite is assumed, an

Table 1. Measurement conditions. Soller slit angle is 5 degrees for No. 1–11 and 2.5 degrees for No. 12–22.

No.	1,12	2,13	3,14	4,15	5,16	6,17	7,18	8,19	9,20	10,21	11,22
Scan mode	cont.	step	cont.	cont.	cont.	step	cont.	cont.	cont.	cont.	cont.
Step[deg]	0.02	0.02	0.01	0.05	0.1	0.1	0.05	0.05	0.05	0.05	0.05
DS,SS[deg]	2/3	2/3	2/3	2/3	2/3	2/3	2/3	2/3	2/3	1/3	1
RS[mm]	0.1	0.1	0.1	0.1	0.1	0.1	0.05	0.2	0.3	0.1	0.1



(a)



(b)

Fig. 7. Results of (a) crystallite size and (b) strain for ZnO nanocrystalline under 22 instrumental conditions (Table 1). Horizontal axis expresses the condition number.

ellipsoidal crystallite model is more appropriate than a spherical model.

Next, we check the dependence of the results for the experimental conditions. One of the merits of the FP method is that the results are not influenced by experimental conditions without correction from the standard sample observation. Reproducibility of the

results should be checked. In the Table 1, the 22 types of measurement conditions are summarized. Here, we change the angular apertures of the Soller slit, scan mode (continuous scan or step scan), apertures of divergence slit (DS) and scattering slit (SS), and receiving slit (RS) width. Soller slit angle is 5 degree for No. 1–11 and 2.5 degree for No. 12–22.

Results are shown in Fig. 7. (a) is a plot of the volume averaged mean diameter perpendicular to *c*-axis direction. (b) is that of lattice strain. Horizontal axis is the condition number. Their error bars show the estimated standard deviations (1 sigma) of the least square refinement. It is shown that the values are comparable to their standard deviation with a high degree of reproducibility.

5. Summary

In this report, crystallite size, size distribution and strain studies using the FP method implemented in PDXL 2 and its underlying theory are described. The results obtained by analyzing the data of the size-strain round robin are almost consistent with of the data in the round robin report. We also apply the FP method to analysis of ZnO nanocrystalline and find that the ellipsoidal crystallite model is more suitable to explain the experiment and check the reproducibility of the results under multiple experimental conditions. This report finds that the reproduced analysis results were in agreement with estimated standard deviations.

In PDXL 2, more reliable analysis results can be obtained much easier than the ordinary method, which require the use of standard samples. We hope that PDXL will be utilized for material developments and contribute to the progress of material science.

References

- (1) R. W. Cheary and A. Coelho: *J. Appl. Cryst.*, **25** (1992) 109–121.
- (2) *The Rigaku Journal (English version)*, **28** (2012), No. 1, 29–30.
- (3) J. I. Langford and A. J. C. Wilson: *J. Appl. Cryst.*, **11** (1978), 102–113.
- (4) *The Rigaku Journal (English version)*, **25**, (2008), No. 1, 23–24.
- (5) D. Balzar, N. Audebrand, M. R. Daymond, A. Fitch, A. Hewat, J. I. Langford, A. Le Bail, D. Louër, O. Masson, C. N. McCowan, N. C. Popa, P. W. Stephens and B. H. Toby: *J. Appl. Cryst.*, **37** (2004), 911–924.
- (6) R. Delhez *et al.*: *The Rietveld Method*, Ed. by R. A. Young, Oxford University Press, (1995), 136.
- (7) B. E. Warren and B. L. Averbach: *J. Appl. Phys.*, **21** (1950), 595–599.
- (8) B. E. Warren and B. L. Averbach: *J. Appl. Phys.*, **23** (1952), 497.
- (9) P. Scardi and M. Leoni: *J. Appl. Cryst.*, **32** (1999) 671–682.